The Effect of Polymethylsilsesquioxane Concentration on The Liquid Foundation: Characterization of Nanostructure and Biophysical Properties

ABSTRACT

Aims: Polymethylsilsesquioxane (PMQS) is a silicone derivative that serves as a skin conditioning agent and moisturizer in cosmetics. The objective of this study is to identify the effect of different concentrations PMSQ (0.12, 0.20 and 0.35 wt %) on liquid foundation (LF) and find the optimized composition *in vitro*.
Study design: Structural and morphological features of the examined nano/micro-sized samples were investigated by different methods.
Place and Duration of Study: Hacettepe University, Department of Physics Engineering, X-Rays Laboratory, between September 2017 and September 2019.
Methodology: Micro/nano scale structural and morphological properties of samples were investigated by means of a multi-methodological approach based on Small- and/or Wide-Angle X-ray Scattering (SWAXS), Scanning Electron Microscopy with Energy Dispersive X-ray Spectroscopy (SEM/EDX), Attenuated Total Reflection-Fourier Transform Infrared (ATR-FTIR) Spectroscopy and UV-*vis* Spectroscopy. The LF (control) and PMSQ-LF films at one-week intervals for four weeks, and bovine leather coated samples with LF and PMSQ-LF were also investigated by SWAXS. The effect of PMSQ on biofilm formation activity in E. coli and S. aureus were also examined.
Results: The most significant finding of this study is that even the low concentration of polymer in LF showed differences in nano structure and it was found that a decrease in biofilm formation. Nano formation becomes more pronounced, and the number of agglomerations decreases after 4 weeks. The reason for the study over a 4-week period was the desire to take into account the independent effect of each LF use, as well as the periodic stacking and diffusing effect that will occur in the depths of the skin over time. In the UVA range (320-400 nm) lower transmittance values were found for LF and PMSQ - LF films. **Conclusion:** The results suggest that optimum polymer concentration in liquid foundation should be considered as a main step. The smart and systematic use of polymer additives is directly manifested in the nansoscopic structure and can improve the harmful UV rays prevention properties, which are important for health as well as cosmetic effects for beauty purposes.

Keywords: PMSQ polymer, Liquid foundation, SAXS / WAXS, Spectroscopy, Biofilm

1. INTRODUCTION

Nanomaterials are widely used in cosmetic products due to their different and diverse effects. The formation and use of new nanomaterials are necessary to design, develop and explain features such as the product's stability, skin absorption potential, route of exposure and formulation of cosmetic products. The concept of “nanomaterial” defined in cosmetics is defined as insoluble, stable nanoparticles like polymers that can enter the body and cause direct health/safety problems.

Especially, nanoparticles size and stabilities very important to use for skin. Polymers have the advantage of relatively small size and stability and may be soluble or insoluble nanoparticles depending on their structure. As is known today, nanomaterials can exhibit unique/superior biochemical properties compared to micro particles of the same chemical. Because, as the mass shrinks in the nanomaterial, the surface area increases and the electrons in the atoms begin to

show quantum mechanical properties beyond the conventional properties. Thus, the unique chemical properties achieved can result in unique bioactivities [1]. Briefly, the material particle is stripped from nano-sized macro features and behaves with very different probabilities with its quantum properties.

Essentials for cosmetic products are foundation products that are perfect for a flawless skin look. The foundation should not spoil the natural appearance and should be brought into a suitable form for dry or oily skin according to the skin type. The expectations are that it never dries the skin, it is not noticed that it corrects the natural image and it creates a homogeneous and non-spillable form without allowing different color tone during the application phase. While special additives in the foundation compensate for moisture loss, it ensures uniform distribution of colored pigments and increases the durability and stability of the foundation [2].

Polymethylsilsesquioxane (PMSQ) polymer (Fig. 1) is one of the common polymers used in cosmetic products due to its outstanding properties such as thermal stability, non-toxicity, water resistance, ease of processing in powder applications and film forming [3,4]. It has been widely used for hair (shampoos, hair creams and style), skin (facial care, facial cleansing, body care and baby care) and sun care (sun protection, after sun and spontaneous tanning) products.

As concentration of PMSQ changes, the surface tension, viscosity and density of the nanostructures of the solution also change, and the size of the nano spheres formed in the gel phase increases [5].

Cosmetic companies explain the ingredients in their products, but these formulations are kept confidential. The critical proportions of polymer materials in these products are determined only by molecular analysis and their research and development (R&D) studies without nanoscopic analysis.

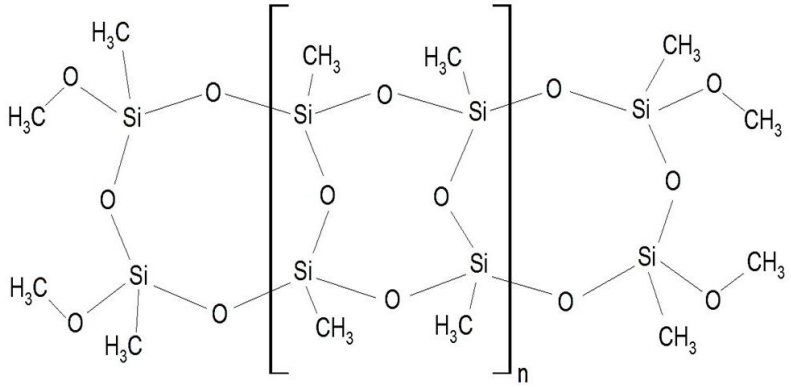

Fig. 1. The chemical structure of polymethylsilsesquioxane [4]

Characterization of the nanoscopic structures formed by different polymer concentration, which is important molecular components used in the cosmetics industry, and the influences of these structures on the properties can be established directly.

In this work, nanostructural and biophysical analyses were conducted on a set of samples formulated by adding PMSQ in LF and evaluating the effects of their concentrations on the structural properties of the systems. The nano- micro scales structural characteristics and morphological properties were investigated by means of a multi-methodological approach based on Small- and/or Wide-Angle X-ray Scattering (SWAXS), Scanning Electron Microscopy with Energy Dispersive X-ray Spectroscopy (SEM/EDX) and Attenuated Total Reflection-Fourier Transform Infrared (ATR-FTIR) Spectroscopy.

It is important that the cosmetic products used are effective against ultraviolet (UV) rays. UV rays cause tanning of the skin. It can penetrate into the dermis layer of the skin and causes aging of the skin [6]. Transmittance characteristics were measured in the UV and visible range from 320 to 700 nm to evaluate the effect of PMSQ concentration.

To determine the effect of different concentration of PMSQ on *E. coli* and *S. aureus* biofilm formation in the presence of PMSQ was measured using crystal violet staining.

With this study, it has been tried to be proved that even a small change of the polymer concentration used in cosmetic products can lead to significant changes in structure-property relationship.

2. MATERIAL AND METHODS

2.1 Materials

PMSQ powder was purchased from Wacker Chemie AG (Germany) and the liquid foundation Wacker 03CC14 (LF) was obtained commercially.

The conventionally finished crust bovine leather (dry, raw and unpainted) was used for the coating with LF.

2.1.1 Preparation of The Films

The control sample (LF-1, in cream-gel form) is the commercially available version of the product that has not been modified with polymer content. The LF with in many different amount of PMSQ polymer were prepared find to the best condition to achieve.

The samples contain PMSQ polymer were prepared by adding polymer in LF as 0.4 mg (LF-2), 0.7 mg (LF-3) and 1.2 mg (LF-4) (with mass percentages of 0.12, 0.20 and 0.35 wt %, respectively), were selected to analyze in this study.

To ensure homogeneous of the gel form samples and spread evenly on the surface, centrifuge and vibrating systems were used.

Four group film samples were prepared for the SAXS-WAXS analyzes, SEM, FTIR spectroscopy and biofilm experiments. To obtain film form, the sample was spread on the 9x6 mm2 special glass substrate by using an additional coverslip, as homogeneous as possible, at an angle of 45° with the surface. The film thickness of the prepared samples was measured as 500-micron by using a compact non-contact 3D surface profiler system.

To obtain information about (time-depended variation), film samples were prepared and kept same environmental factors such as ambient temperature, humidity and light for one month.

For optical transmittance and reflection measurements, 500-micron thick PMSQ- LF films on a 5\times5 mm2 glass substrate were homogeneously prepared with the same technique.

2.1.2 Biofilm formation in bacterial media

Firstly, the bacterial strains (*Escherichia coli ATCC 25922 and Staphylococcus aureus ATCC 25923*) were inoculated into 10 mL BHI broth and the samples were incubated at 37°C for 18 h. Then the bacteria concentrations adjusted to Mc Farland 3. In order to sterilize the treated materials, 70 % ethanol solution and UV were used. 2 mL bacteria solution were prepared in fresh BHI broth and sterilized material were put into the wells of 24 well plates and incubated at 37°C for 18 h. After incubation, samples were washed with PBS buffer (pH 7) for three times and stained with 1 % crystal violet solution for 25 min.

For solubilizing bounded crystal violet on the surface of with and without PMSQ, 70 % ethanol solution was used for 20 min. Optical density (OD) was measured at wavelength 560 nm. Biofilm formation on LF without PMSQ was used as a positive control and biofilm amount accepted as 100 %. Biofilm formation (%) was calculated by using Equation 1.

$$\frac{(OD_{control} - OD_{with\ PMSQ})}{OD_{control}} \times 100 \quad (1)$$

2.2 Characterization Methods

2.2.1 SAXS-WAXS data acquisition and data analysis

Small-angle X-ray scattering (SAXS) and wide-angle X-ray scattering (WAXS) data were collected at HECUS System3 at Hacettepe University, Ankara Turkey and BL23A SWAXS end-station of the Taiwan Light Source (TLS) of the National Synchrotron Radiation Research Center (NSRRC), Hsinchu, Taiwan.

Experimental conditions for the HECUS System3 SWAXS device (He, 2009) are summarized by 50 kV, 40 mA, CuK_{α} characteristic ray (1.54 Å) and measurement time of 400 s for each sample.

SAXS and WAXS data were collected using ASA3 (Amplitude Spectrum Analyzer) software [7-16]. SAXS modeling studies and pair distance distribution function (PDDF) analyzes were performed by importing data from ASA3 into IgorPro 6.37 program in EasySWAXS program [17, 18].

SAXS-WAXS experiments of the control and PMSQ-LF films at one-week intervals for four weeks, and LF and PMSQ-LF applied bovine leather groups were carried out at BL23A SWAXS end-station. During the measurements, 10 keV, which is the appropriate energy value for our samples, was used [19,20].

Scattering intensity, *I(q)* is plotted against q- magnitude of the scattering vector. Then, the PDDs were adjusted to be the smallest chi-square (chi2, χ^2) value, and 3D morphologies of electron density were found in the DAMMIN program [18, 21-23].

Fitted I-q scattering data and PDDF graph of PMSQ polymer and the LF-1 control group was fitted to the Debye-Anderson-Brumberger (DAB) model [18] containing biphasic randomly distributed nanoparticles and the gyration radius (R_g) and maximum width (D_{max}) values were obtained with PDDs. Then, the 3D morphology of the structure was obtained. The LF-2, LF-3 and LF-4 samples fit the Fractal Polycore model [18] from a fractal structure that causes scattering with a diffuse core-shell sphere primary building block.

2.2.1.1 Monitoring the changes of LF samples with time

I-q scatter plots for LF control samples were fitted the Multi-Core Fractal model [18] from a fractal structure causing scattering with a diffuse core-shell sphere primary building block. The LF films contain polymer were fitted the Power Law model [18], which is ideal for relatively mobile fluids such as slippery-thinning, weak gels, and low-viscosity dispersions.

2.2.2 SEM and EDX

The SEM microstructure imaging of samples was performed using an Environmental Scanning Electron Microscope (Quanta 400 F Field Emission SEM) and Energy Dispersive X-ray Spectrometry (EDX) attached to the scanning microscopy system was used for identifying the elemental composition of samples.

2.2.3 ATR-FTIR Spectroscopy

ATR-FTIR spectra of samples were recorded by Perkin Elmer 400 spectrophotometer equipment with attenuated total reflection (ATR) accessory in the range of 4000-450 cm^{-1}. The acquisition parameters were 32 co-added scan and 4.0 cm^{-1} resolution.

2.2.4 Optical measurements

Optical transmittance and reflection measurements were made using a CVI Digichrome 240 monochromator operating with the spectral range from 320 to 700 nm and a BPW34 photodiode.

3. RESULTS AND DISCUSSION

3.1 SEM and EDXS Analysis

The scanning electron microscopy (SEM) with an energy dispersive X-ray spectroscopy (EDX) was used to provide visualization of microstructure and element composition of LF films.

As seen SEM images of four LF films in Fig. 2, surface homogeneity of LF film prepared by adding PMSQ polymer seems to be good. Particularly, in the 5-micron scale images, uniform and homogeneous distribution could be an indication that the PMSQ increase spread smoothly of surface and contributes to the formulation by dissolving properly.

The highest Si and O content was found for LF-3 film from EDX (Supplementary Fig. S1).

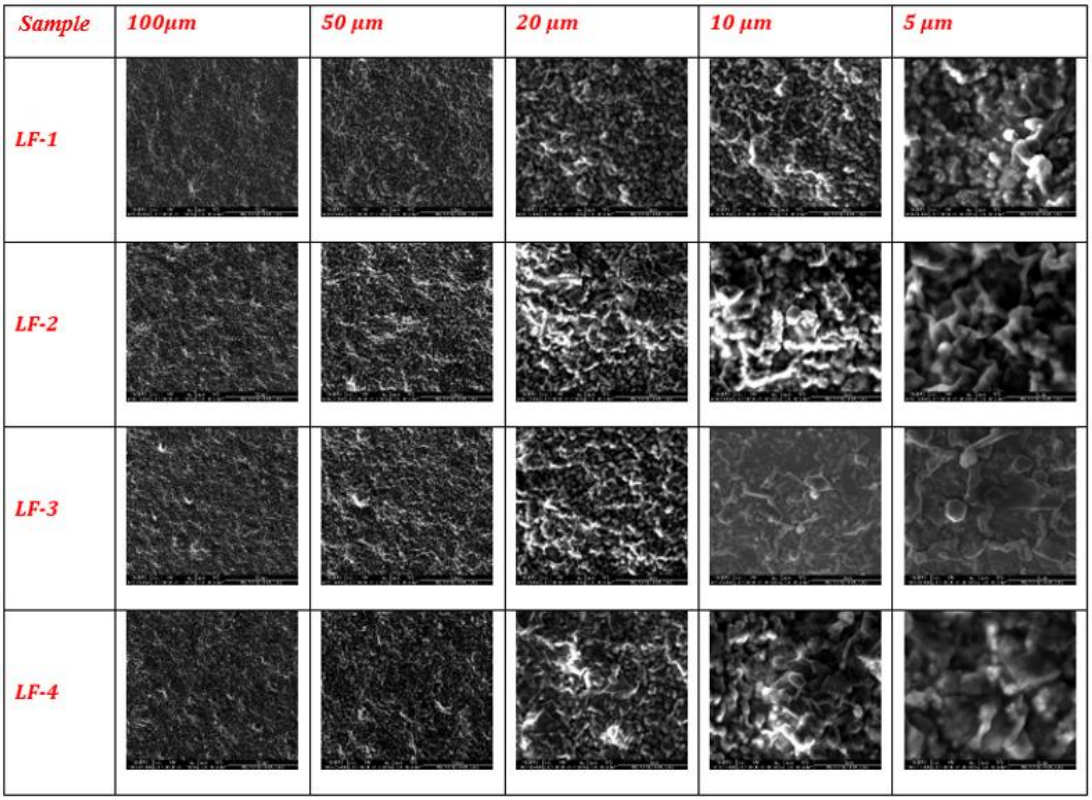

Fig. 2. SEM images of LF control (LF-1) and PMSQ-LF films (LF-2, LF-3 and LF-4)

3.2 PDDF Calculator Analysis

In order to obtain the distance distribution of the formations in the samples with respect to each other, SEM images of LF films with 10 µm scale (Fig. 2) were selected to easily simulate the real microscopic view and the distance distribution of the formations were calculated by using a PDDF Calculator software [24].

Considering the PDDF calculator analysis shown in Fig. 3 for LF control (LF-1) and PMSQ-LF films (LF-2, LF-3 and LF-4), since the formations on the sample surface do not have homogeneous structural features, the surface nanoscale features of the films vary from one another.

The maximum distance is approximately 420-500 Å. It states the importance and necessity of SAXS analysis beside with SEM analysis. Even if the sample has a complex structure, a 3D uniform distance distribution can be obtained by SAXS, while these distributions obtained in SEM analyzes have irregular distance distributions (Fig. 3).

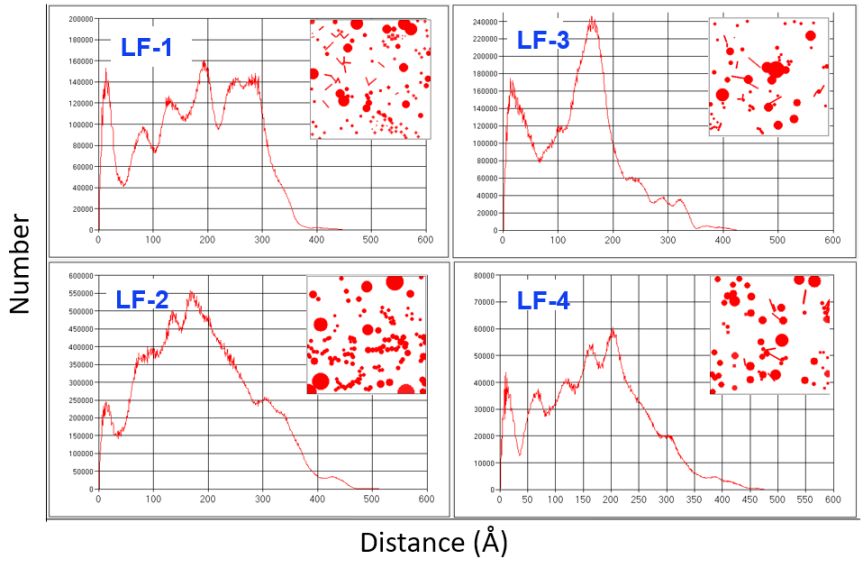

Fig. 3. PDDF plots of LF control (LF-1) and PMSQ-LF films (LF-2, LF-3 and LF-4). using SEM images. The inset in the upper right shows the distance distribution of the formations in the samples

3.3 SAXS Analysis

Fitted I-q scattering and PDDF graph of PMSQ polymer and R_g and D_{max} values of 3D morphology are given in Fig. 4. The PMSQ polymer was fitted to the Debye-Anderson-Brumberger (DAB) model [18] containing biphasic randomly dispersed nanoparticles.

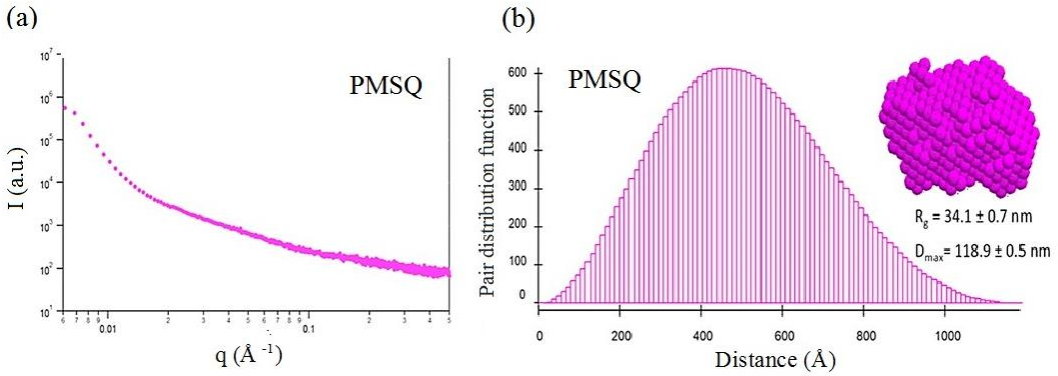

Fig. 4 (a) I-q scatter plot (b) PDDF distribution, 3D morphology, R_g and D_{max} values of PMSQ polymer

3D morphology of PMSQ polymer is uniform and its shape close to spherical. However, morphology alone is not enough, PDDF distribution is also very important.

To compare with a similar SAXS study on PMSQ by Lee et al. [25] the SAXS profile (log-log) of the PMSQ polymer was plotted and the slope of the Porod region was found to be α= -1.43 (Fig. 5a) and Kratky plot was drawn (Fig. 5b) which gives information about the conformation of polymer chains.

PMSQ, which is prone to the formation of spherical morphologies at the nanoscale, is widely used in many different research due to its biocompatible properties and interesting physical, chemical and pharmacological properties [26,27]. Lee et al. [25] also synthesized PMSQ with step-like structure and characterized them by SAXS analysis. There is a continuous upward trend in Kratky plot of the PMSQ polymer. This result reveals that an unfolded polymer chain expresses random formation.

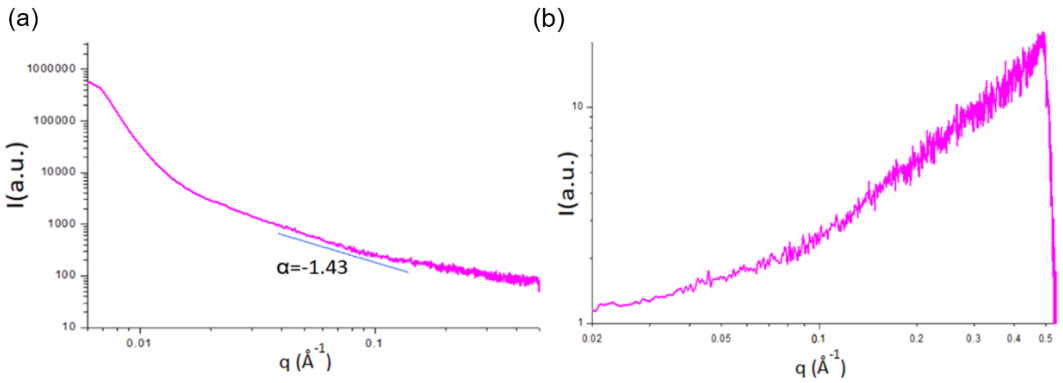

Fig. 5. (a) SAXS profile and the slope of the porod region (b) Kratky plot of PMSQ polymer

SAXS analyzes of the pure and polymer LF films were also carried out in detail. Fitted I-q scattering and PDDF distribution, 3D morphology, R_g and D_{max} values of control (LF-1) and PMSQ-LF films (LF-2, LF-3 and LF-4) are shown in Fig. 6. The gyration radius and scattering intensity increase as PMSQ is added to the LF films. In the LF-4 film, the intensity has decreased compared to the others. It means that the increased PMSQ amounts are also causing more X-ray scattering effect from the sample with the increased size of the nanoglobules in LF-4. The R_g value increases generally and regularly with the increase of the PMSQ concentration.

In addition, the 3D morphology of the electron density of the LF films is very close to a sphere. This result reveals that, nanoscale polymer contribution is very homogeneous inside of the 3D bigger micro-clusters. In micro scale adsorption is appearing while in nano level, the formation of nanoglobules and the dispersion are possible and uniform distribution appears. Deviation from the 3D spherical formation toward the bigger PMSQ amounts also increases X-ray scattering intensity.

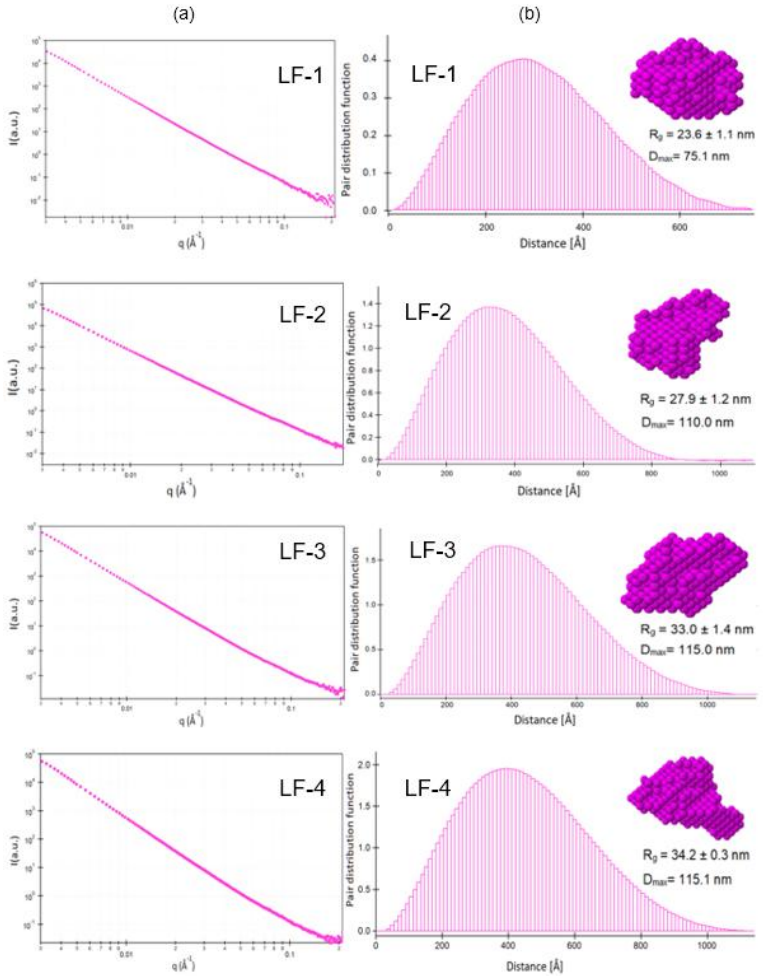

Fig. 6. (a) I-q scatter plots (b) PDDF distribution, 3D morphology, R_g and D_{max} values of LF-1 control and PMSQ-LF films (LF-2, LF-3 and LF-4)

To find the effect of time on the LF-1 (control) and polymer-LF films (LF-2-LF-4), SWAXS experiments were also performed at the NSRRC-BL23A SWAXS beamline. The time variation of fitted I-q scattering, PDDF distribution, 3D morphology, R_g and D_{max} values of polymer–LF-3 film (as a representative) is given in Supplementary Fig. S2.

The highest R_g value was found after four weeks for the polymer- LF films and the scattering intensity decreased (Fig. S2). In other words, the number of agglomerations decreases after 4 weeks for the increase of the overall size. In addition, nano-formations diminish from each other by increasing their size with the effect of drying. The increase in R_g value can be explained by the fact that the large-scale aggregation becomes more pronounced, that is, the higher electron density concentration in the gel structure in which this nano formation is located. With this part of the study, it was obtained that the usage time limits are big possibly depend on polymeric behavior in chemical content for these type cosmetic products. So, the shelf life of cosmetic products should be determined according to controlling of these nano structural changes.

The I-q graphs of LF and PMSQ-LF applied on the bovine leather were plotted in Fig. 7. The LF-1 leather (control) fits the Fractal model [18] which allows combining two volume and two mass fractals, while for three PMSQ-LF samples on leather, polydisperse spheres, were calculated from a fractal structure with a primary building block and Spherical Fractal (Fractal Polysphere) model [18] is fitted. The characteristic laying structure is revealed from the periodic scattering peaks, corresponding to a d-spacing of 10.8 nm, which structure is stable with the different PMSQ concentrations studied.

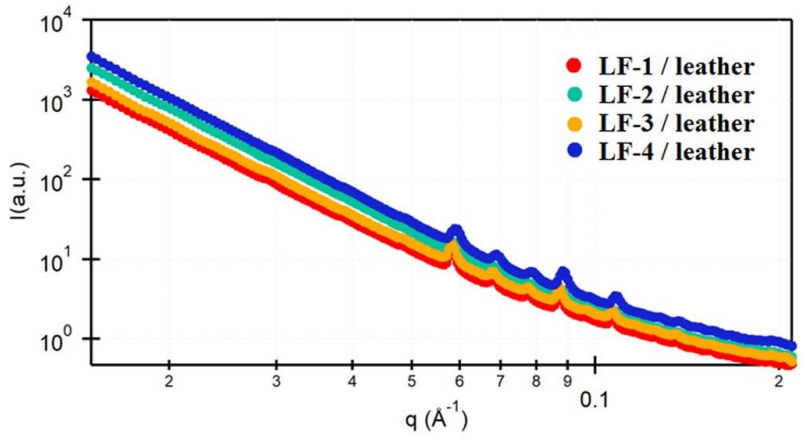

Fig. 7. Comparison of model-fitted I-q scatter plots for bovine leather coated with LF and PMSQ-LF (LF-1 control and PMSQ-LF (LF-2, LF-3 and LF-4) samples

3.4 WAXS Analysis

Using WAXS measurements can be obtained information about the crystal structure of the samples. The results obtained from WAXS reveals that as PMSQ content increase in LF, WAXS pattern is also changing and Bragg peaks are sharpening (Fig. 8). However, the highest content of PMSO weakens the crystalline structures substantially.

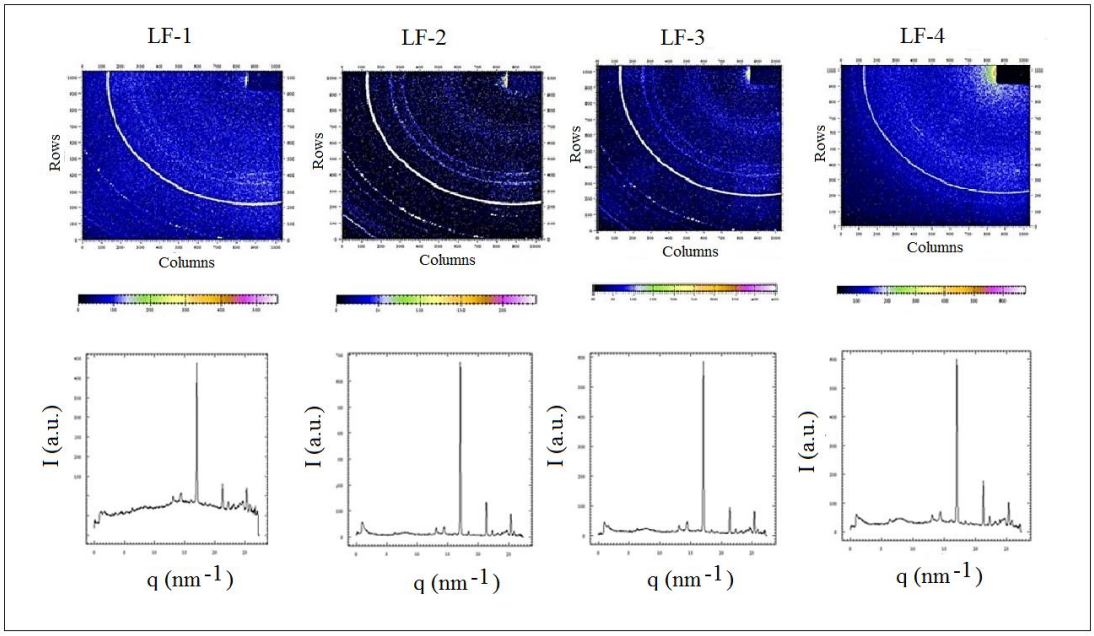

Fig. 8. WAXS images and I-q graphs for control (LF1) and PMSQ -LF films (LF-2, LF-3 and LF-4)

It was concluded that the crystallization increased regularly in the structure with the increased PMSQ. WAXS images and graphs for LF with 0.7 mg PMSQ (LF-3) after 1st, 2nd, 3th and 4th weeks and applying LF on bovine leather are given in Supplementary Figures S3 and S4, respectively. According to the WAXS results of both groups we can say that the polymer adding to LF only increased the intensity which support the increased number of crystallographic regions.

3.5 ATR-FTIR spectral analysis

Changes of the infrared band intensities and/ or wavenumbers (cm^{-1}) of LF samples with different concentration of PMSQ were investigated using ATR-FTIR spectroscopy. Fig. 9 shows ATR-FTIR spectra in the wavenumber range from 4000 to 450 cm^{-1} for the LF-1 (control) and PMSQ -LF films (LF-2, LF-3 and LF-4). The observed band wavenumbers in the ATR-FTIR spectra of all samples and the assignments of the main bands are given in Table S1.

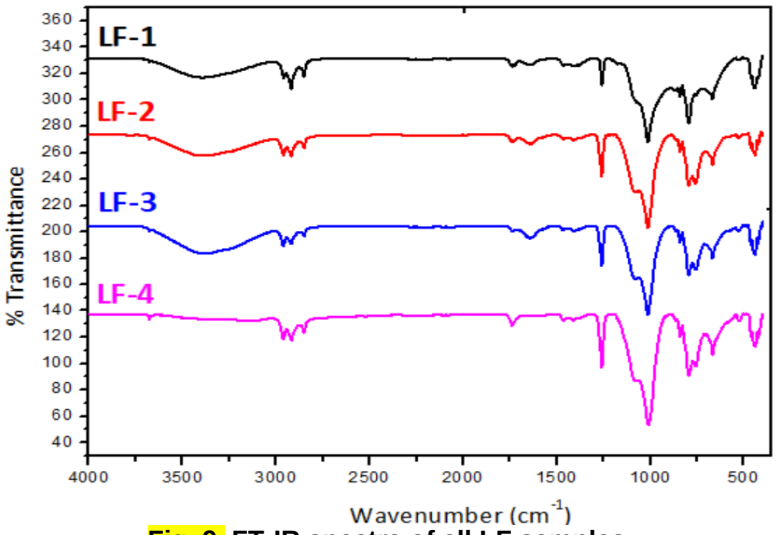

Fig. 9. FT-IR spectra of all LF samples

PMSQ contains Si-O-Si linkages and also Si-CH_3 groups (Fig. 9). The Si–CH_3 groups result in a hydrophobic effect in LF. The observed band at 3393 cm^{-1} is characteristic of OH and/or Si-OH stretching vibrations. The bands at 2959 cm^{-1} and 2918 cm^{-1} are characteristic of stretching vibrations of C-H bonds in Si-CH_3.

The bands at 1414 cm^{-1} and 1259 cm^{-1} are attributed to the bending vibrations of CH_3 group in Si-CH_3. The medium intense band at 1070 cm^{-1} and a strong, sharp band at 1013 cm^{-1} are due to Si-O-Si stretching of the PMSQ. The observed bands at 795 cm^{-1} and 754 cm^{-1} in the ATR-FTIR spectra of the LF films are attributed to the Si-C stretching vibrations [25, 28,29].

The 1739 cm^{-1} band corresponds to the stretching of the C=O ester carbonyl or carboxylic acid groups, which are characteristic of fatty acids. The band at 1645 cm^{-1} can be results from the C=O stretching in LF. It is apparent that from ATR-FTIR spectra of LF samples (Fig. 9) with the different concentration of PMSQ have little differences between control (LF-1) and PMSQ-LF samples, i.e. there is no obvious regular wavenumber shift. However, the intensities of some of infrared bands of LF-1 control sample such as 3393 cm^{-1}, 1259 cm^{-1}, 1070 cm^{-1}, 1013 cm^{-1} and 795 cm^{-1}, possess particular features in addition of PMSQ.

With increase of the concentration of PMSQ, the band intensity of 3393 cm^{-1} slightly increases for LF-3 which indicated increasing water retention. This band is disappeared in the ATR-FTIR spectrum of LF-4 film formed by PMSQ (0.35 wt %) which has excellent water-repellency. Hydroxyl groups in the cosmetic products are playing important roles in macromolecular folding of PMSQ and molecular and intermolecular O-H interactions are effective on biophysical properties.

The band intensities increase very little of the other bands mentioned above. However, band intensities of these vibrational modes increase in LF-4 sample with the 0.35 wt % PMSQ which can effectively inhibit the diffusion movement of the PMSQ chain.

3.6 Optical properties

The reflectance and transmittance spectra of LF samples are shown in Fig. 10. The studied range of wavelengths covers from 320 nm to 700 nm, that is UVA and visible spectrum.

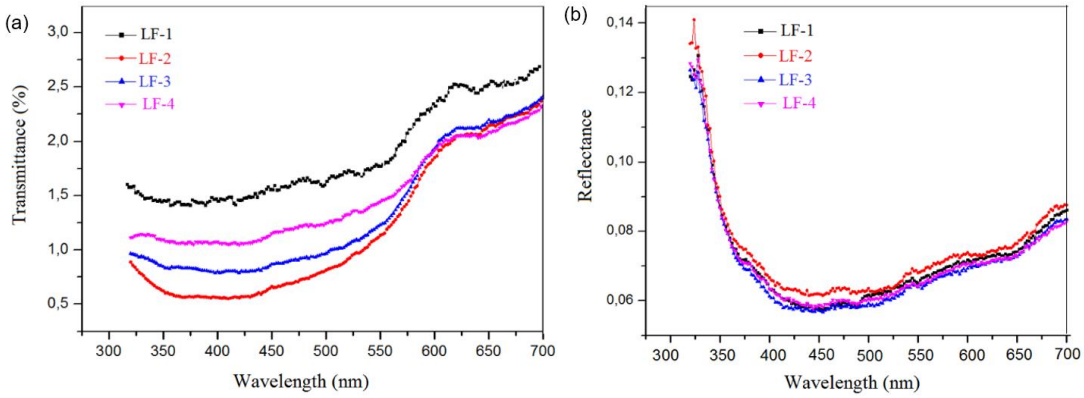

Fig. 10. (a) Optical reflection graph of LF samples (b) optical transmittance graph of LF samples

In general, lower transmittance values or low absorbance for all samples were observed both in the ultraviolet and in the visible range. Decrease in transmittance with increasing PMSQ concentration was observed for the PMSQ-LF samples (Fig. 10 a) compared with the control sample (LF-1). In the range of UVA, the transmittance is decreased greater than in the visible range.

The LF-2 (PMSQ; 0.12 w %) has minimum UV transmittance between 350-425 nm. This result reveals that a slight increase in the polymer ratio can significantly change the optical properties.

3.7 Biofilm Analysis

To determine the effect of different concentration of PMSQ on *E. coli* and *S. aureus* biofilm formation of 18 h formed in the presence of PMSQ was measured using crystal violet staining.

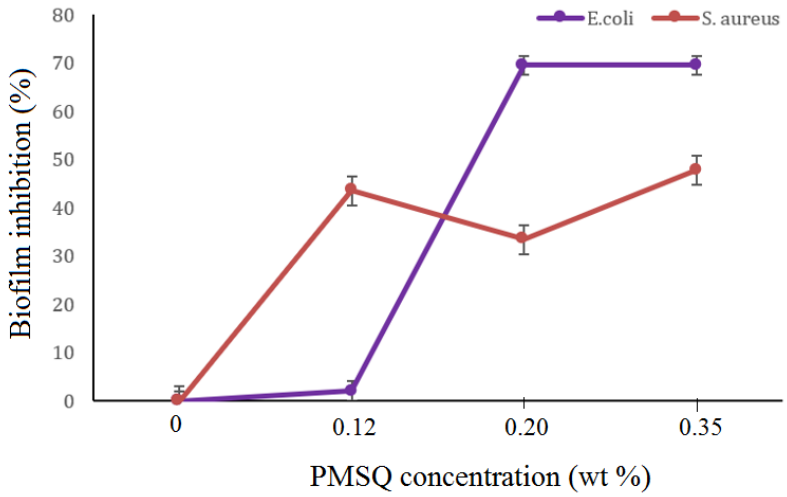

Fig.11. Inhibition of biofilm formation at different concentrations of PMSQ on *E. coli* and *S. aureus*

The finding of this study showed that the samples containing PMSQ caused reduction in biofilm formation capability of *E. coli* and *S. aureus*, when compared with the control (Fig. 11). The antimicrobial effect of samples increases with increasing concentrations of PMSQ.

Biofilm inhibition (%) values have been measured for *E.coli* (80 μg/mL) and *S.aureus* (70 μg/mL) as >99% in a previous study which is related to highly antibacterial biocompatible AgNPs [30].

In the present study, the samples containing 0.20 wt % PMSQ significantly reduced the biofilm formation of *E. coli* (the biofilm inhibition is 70%) while the lower inhibition effect (40-50%) was observed against *S. aureus* biofilm formation even at highest concentration of PMSQ. On the other hand, even the lowest concentration showed inhibitory effect on biofilm formation of *S. aureus* with 43.5% inhibition level while any significant inhibition cannot be observed *for E. coli* in that

concentration. The findings indicated that the bioactive properties of the biocomposites containing polymer such as PMSQ can be used for cosmetic purposes.

The cationic–hydrophobic balance, cationic and hydrophobic moieties in molecular structure of these polymers are known to have a major effect on the antimicrobial activity [31-39]. The antibacterial activity of the PMSQ polymer leads to its identification as a potential cell-selective antibacterial agent against *S.aureus* and also *E.coli*. It can be easily adapted to applications, such as coatings and used to sterilize various surfaces, inclusively those of medical instruments.

4. CONCLUSION

Polymeric materials are critically important to the creation of modern cosmetics and personal-care products. Coating ability of polymers is widely used in creams, glasses, nail paints, etc. in cosmetic industry. The coating includes polymer matrix or binding polymer. Polymer components included by cosmetic products can cause interestingly and easily spread and handled [38].

Over the last decades, more research is focused on newly designed foundations which have functional coating properties that show faster drying rate, self-healing, easy to clean, antibacterial, antifouling, low water permeability, and less moisture retention. The nano scale investigations on polymer components' microemulsion, their physico-chemical/biophysical properties can be attained by SAXS method and the other complementary conventional techniques.

In this study, we used extensive techniques for the characterization of nano/ micro structure, the morphological data/chemical composition, UV-protection and biofilm formation. SAXS and WAXS data was used to understand the crystalline and nanostructures for information about the particle size and distribution of cosmetic grade PMSQ with different concentration in LF at nano-scale. We found that the structure of the LF changes noticeably with the polymer concentration.

The two-dimensional SAXS patterns and WAXS images of the LF (control) and PMSQ-LF films, PMSQ -LF-3 film after 1^{st}, 2^{nd}, 3^{th} and 4^{th} weeks and LF (control) and PMSQ-LF on bovine leather were also investigated to reveal the performance of anti-bacteria. The intensities of the O-H stretching band of hydroxyl groups, Si-O-Si and Si-C stretching bands in the ATR-FTIR spectra of the samples increase specially in LF-4 sample with the 0.35 wt % PMSQ which can effectively inhibit the diffusion movement of the PMSQ chain. It can be explained by large molecular volumes, which likely decrease the potential for this ingredient to penetrate the skin significantly. Within the limitations of this study, it can be concluded that the LF combined with 0.20 % wt PMSQ showed a significant antimicrobial activity against E. coli and S. aureus biofilm.

The polymers and other commonly used macromolecular materials in cosmetic field must be control at the nanoscale. Within the scope of this article, it has been revealed that even small changes in polymer concentration lead to visible nanoscopic structure differences, and these nanostructures are effective on antibacterial properties and UV protection.

Due to the increase in polymer concentration in cosmetic products, unexpected results can be seen in their properties. It is important to note that the formation of nano structures that can occur self-assembly in polymer and other macromolecular structures (which are already present in the content of cosmetic products) should be consciously taken under the nanoscopic scaled controls.

The type of polymer and the ingredients of the foundation affect the miscibility, solubility and homogeneous distribution of the polymer [38]. In other words, the functional coating effects of the product in foundation formulations can be examined with detailed experimental studies with time resolved SAXS analyses. In the future, we intend to study more systematically with the different concentration regime in order to classify the dynamical and structural behavior of polymer in LF and other cosmetic materials. In a further stage of the study, it is also planned to carry out studies on the solubility parameters of the polymer component.

ACKNOWLEDGEMENTS

This study was supported by Taiwan National Synchrotron Beam Research Center, Project Number: 2019-1- Type 146-1: PEC and Hacettepe University Scientific Research Projects Coordination Unit. Project Number: FYL-2018-17456.

COMPETING INTERESTS

The authors have no conflicts of interest to declare that are relevant to the content of this article.

AUTHORS' CONTRIBUTIONS

All authors contributed to the study conception and design. Semra İde designed and directed the study, planned the experiments, contributed to the interpretation of the results. Material preparation, data collection and analysis were performed by Pınar Kaya, Semra İde, Akın Bacıoğlu, Sevgi Haman Bayarı, Chun-Jen Su, Bing-Jun Lian and Sinem Diken Gür. The first draft of the manuscript was written by Pınar Kaya and Semra İde. Semra İde, User Jeng and Sevgi Haman Bayarı reviewed and edited the final version of the manuscript.

REFERENCES

1. Katz LM, Dewan K, and Bronaugh RL. Nanotechnology in cosmetics. Food Chem. Toxicol. 2015;85 127-137.
2. Anonymous. Wacker Chemie AG. Make-Up. Accessed 10 July 2019. Available: https://www.wacker.com/cms/en/industries/consumer .
3. Clarson SJ, Semlyen JA. Siloxane polymers. Prentice Hall. PTR;1993.
4. Baatti A, Erchiqui F, Bébin P, Godard, and Bussières DA. Two-step Sol-Gel method to synthesize a ladder polymethylsilsesquioxane nanoparticles. Advanced Powder Technology. 2017;28(3) 1038-1046.
5. Kucuk I, & Edirisinghe, M. Microfluidic preparation of polymer nanospheres. J Nanopart Res. 2014;16(12) 1-9.
6. Perincek SD, Duran K, Körlü AE, Bahtiyari MI. Ultraviolet Technology. Textile and Apparel. 2007;17(4) 219-223.
7. Glatter O and Kratky O. Small angle x-ray scattering. Academic press, London;1982.
8. Kratky O, and Porod G. Röntgenuntersuchung gelöster fadenmoleküle. Recueil des Travaux Chimiques des Pays-Bas. 1949; 68(12) 1106-1122. German.
9. Hayter JB, and Penfold J. An analytic structure factor for macroion solutions. Mol. Phys.1981;42(1) 109-118.
10. Guinier A and Fournet G. Smal angle scattering of x-rays. Wiley, New York;1955.
11. Li T, Senesi AJ, Lee B. Small angle X-ray scattering for nanoparticle research. Chem.Rew. 2016;116(18) 11128-11180.
12. Kazan U. Bazı Tek ve Çok Katmanlı İnce Film Yapıların X-Işını Saçılma ve X-Işını Kırınımı Yöntemleri ile İncelenmesi. Yüksek Lisans Tezi (master's thesis). Hacettepe Üniversitesi Fen Bilimleri Enstitüsü. 2012. Turkish.
13. Putnam C D, Hammel M, Hura GL, Tainer JA. X-ray solution scattering (SAXS) combined with crystallography and computation: defining accurate macromolecular structures, conformations and assemblies in solution Q. Rev. Biophys. 2007;40(3) 191-285.
14. Allen J, Campbell R, Bakker M, Schad R, Lee DR, Li X, Wang J. Grazing Incidence Small Angle X-ray Scattering (GISAXS) Study of Mesoporous Silica Thin Films on Metal Substrates. JOSHUA,2010; 7 3-8.
15. Nyman M, Fullmer L. Small angle X-ray scattering of group V polyoxometalates. In: Ruhlmann L, Schaming D. (Eds.) Trends in Polyoxometalates Research. Nova Science Publishers Inc. 2015; 151-170.
16. Liu H, Zwart PH. Determining pair distance distribution function from SAXS data using parametric functionals. J. Struct. Biol. 2012;180(1) 226-234.
17. Ilavsky J, Zhang F, Andrews RN, Kuzmenko I, Jemian PR, Levine LE, Allen AJ. Development of combined microstructure and structure characterization facility for in situ and operando studies at the Advanced Photon Source. J. Appl. Crystallogr.2018;51(3) 867-882.

18. Kline SR.Reduction and analysis of SANS and USANS data using IGOR Pro. J. Appl. Crystallogr. 2006;39(6) 895-900.
19. Anonymous. NSRRC. What is Synchrotron Radiation? Accessed 10 July 2019. Available: https://www.nsrrc.org.tw/english/lightsource.aspx .
20. Jeng U, Su, CH, Su CJ, Liao KF, Chuang WT, Lai YH, Liang K S. A small/wide-angle X-ray scattering instrument for structural characterization of air–liquid interfaces, thin films and bulk specimens. J. Appl. Crystallogr.2010; 43(1) 110-121.
21. Franke D, Svergun DI. DAMMIF, a program for rapid ab-initio shape determination in small-angle scattering. J.Appl. Cystallogr. 2009;42(2) 342-346.
22. Konarev PV, Petoukhov MV, Volkov VV, and Svergun DI. ATSAS 2.1, a program package for small-angle scattering data analysis. J. Appl. Crystallogr. 2006;39(2) 277-286.
23. Semenyuk AV, and Svergun DI. GNOM–a program package for small-angle scattering data processing. J. Appl. Crystallogr. 1991;24(5) 537-540.
24. Bayirli A. Examination of metallic alloy implants produced by selective laser melting method via X-ray scattering methods and improvement of production parameters. Doctorate Thesis. Hacettepe University. Ankara;2016. Turkish.
25. Lee HS, Choi SS, Baek KY, Hong SM, Lee EC, Lee JC, Hwang SS. Synthesis and structure characterization of ladder-like polymethylsilsesquioxane (PMSQ) by isolation of stereoisomer. Eur. Polym. J. 2012;48(6) 1073-1081.
26. Quintanar-Guerrero D, Allémann E, Fessi H, and Doelker E. Preparation techniques and mechanisms of formation of biodegradable nanoparticles from preformed polymers. Drug Dev Ind Pharm. 1998;24(12) 1113-1128.
27. Xu JH, Dong PF, Zhao H, Tostado C P, Luo GS. The dynamic effects of surfactants on droplet formation in coaxial microfluidic devices. Langmuir. 2012;28(25) 9250-9258.
28. Hu N, Rao Y, Sun S, Hou L, Wu P, Fan S, and Ye B. Structural evolution of silica gel and silsesquioxane using thermal curing. Appl. Spectrosc. 2016;70(8) 1328-1338.
29. Park ES, Ro HW, Nguyen CV, Jaffe RL, Yoon DY. Infrared spectroscopy study of microstructures of poly(silsesquioxane)s. Chem. Mater. 2008; 20 1548- 1554.
30. Mohanta YK, Biswas K, Jena SK, Hashem A, Abd Allah EF, Mohanta TK. Anti-biofilm and Antibacterial Activities of Silver Nanoparticles Synthesized by the Reducing Activity of Phytoconstituents Present in the Indian Medicinal Plants. Front Microbiol. 2020; 11:1143
31. Schmidt A, Bénard S, and Cyr S. Hospital cost of staphylococcal infection after cardiothoracic or orthopedic operations in France: a retrospective database analysis. Surg. Infect. 2015;16 428–435.
32. Thoma LM, Boles BR, Kuroda K. Cationic methacrylate polymers as topical antimicrobial agents against Staphylococcus aureus nasal colonization. Biomacromolecules. 2014;15(8) 2933-2943.
33. Engler AC, Wiradharma N, Ong ZY, Coady DJ, Hedrick JL, and Yang YY. Emerging trends in macromolecular antimicrobials to fight multi-drug-resistant infections. Nano Today. 2012; 7(3) 201-222.
34. Kuroda K, and Caputo GA. Antimicrobial polymers as synthetic mimics of host-defense peptide. Wiley Interdiscip. Rev. Nanomed. Nanobiotechnol. 2013;5 49-66.
35. Munoz-Bonilla A, Fernández-García M. Polymeric materials with antimicrobial activity. Prog. Polym. Sci. 2012;37(2) 281-339.
36. Vert M, Doi Y, Hellwich KH, Hess M, Hodge P, Kubisa P, Schué F. Terminology for biorelated polymers and applications (IUPAC Recommendations 2012). Pure Appl. Chem. 2012;84(2) 377-41.
37. Watnick P, Kolter R. Biofilm, city of microbes. J. Bacteriology. 2000;182(10) 2675-2679.

38. Li P, Li X, Saravanan R, Li CM, Leong SSJ. Antimicrobial macromolecules: synthesis methods and future applications. Rsc Advances. 2012;2(10) 4031-4044.
39. Sharma D, Rawat M, Sharma J, Ahuja S, Chandra A, Barman S, Arya RK. Polymer coating methods. Rangappa SM. Parameswaranpillai J, Siengchin S. (Eds.) Polymer coatings technology and applications. CRC Press., New York: Boca Raton, Taylor and Francis; 2020.

Supplementary Figures

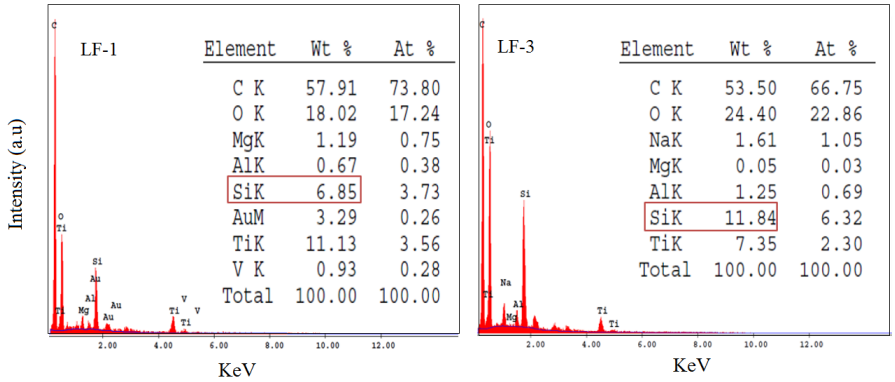

Fig. S1. Energy dispersive X-ray EDX spectra and the tabulated results of LF-1 and LF-3 film samples. (Wt % Weigth *percent*. and At %: Atomic percent)

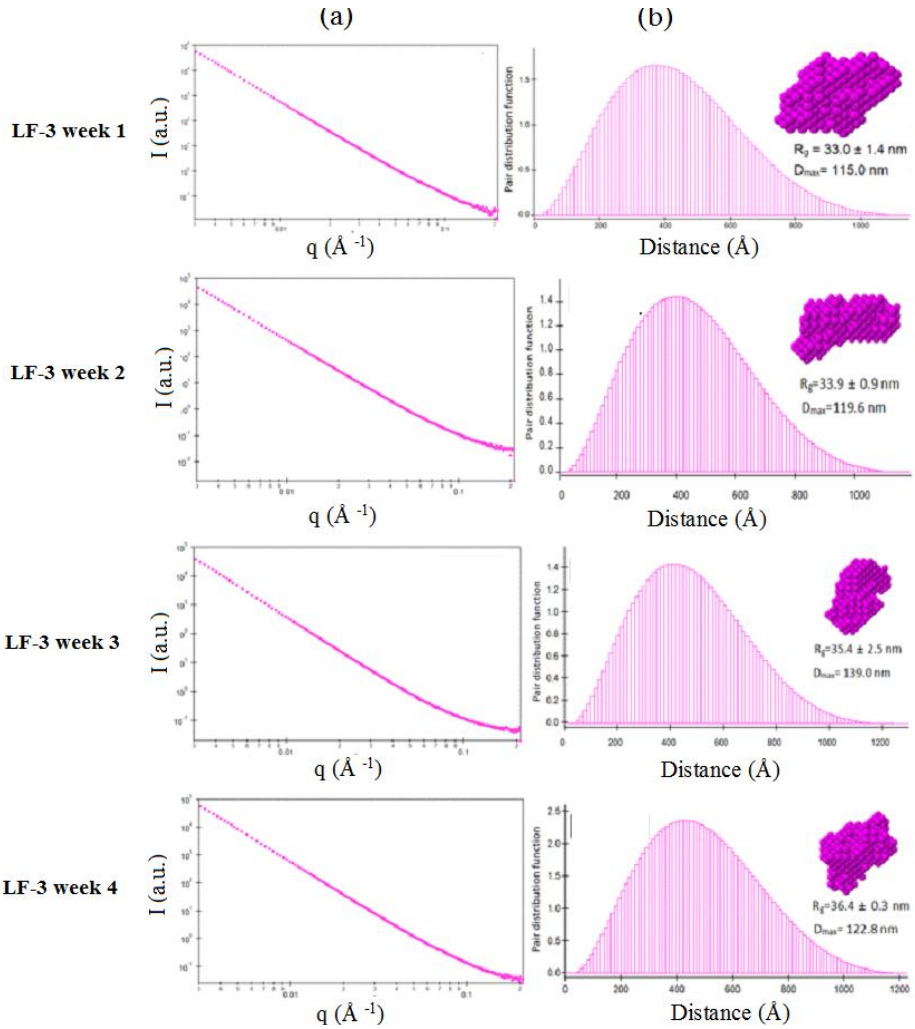

Fig. S2. (a) I-q scatter plots at *weekly intervals for 4 weeks* PDDF distributions (b) 3D morphology, R_g and D_{max} values for LF-3 film.

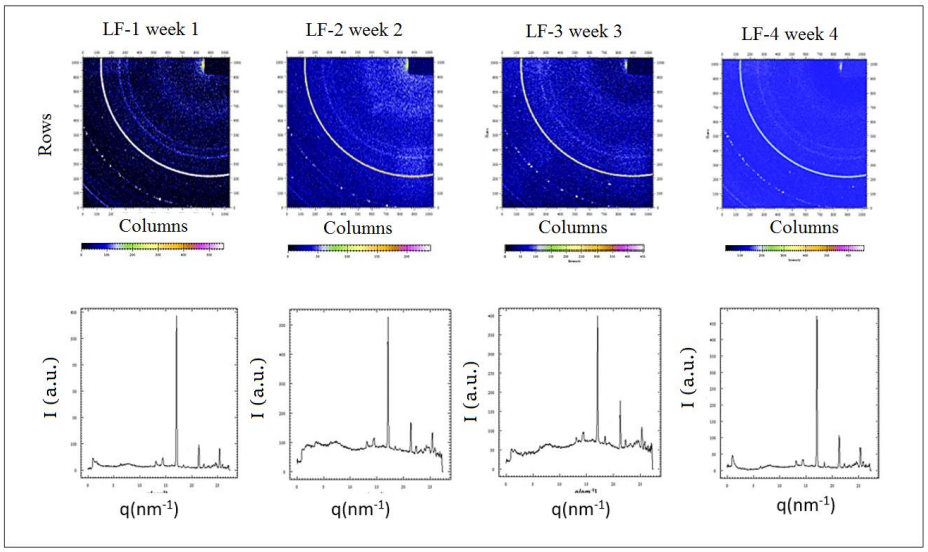

Fig. S3. WAXS images and I-q graphs for PMSQ (0.35 %) - LF films (LF-3) after 1.2.3 and 4 weeks

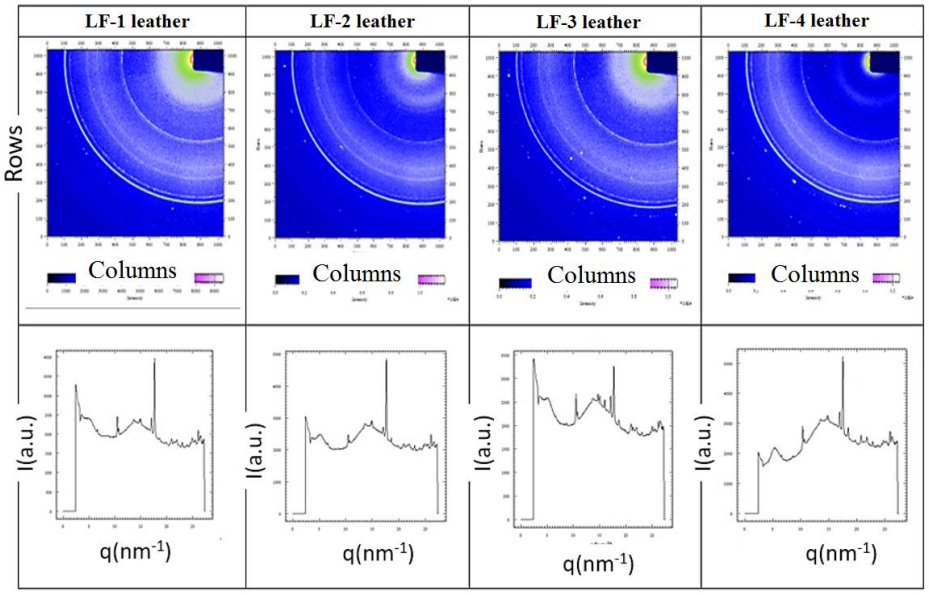

Fig. S4. WAXS images and I-q graphs of bovine leather coated with LF and PMSQ-LF

Supplementary Table

Table S1. Observed wavenumber (cm^{-1}) and and band assignments of ATR-FTIR spectra of LF samples

LF-4	LF-2	LF-3	LF-4	**Assigments** [30-32]
3393	3388	3380	-	O-H stretching and hydrogen-bonded silanols
2959	2961	2961	2961	C-H stretching of CH_3 in Si-CH_3
2918	2918	2919	2918	C-H stretching of CH_2, -CH_3 groups
2851	2850	2851	2850	C-H stretching of CH_2, -CH_3 groups
1739	1738	1737	1738	C=O symmetric stretching
1643	1640	1639	-	C-O and O-H stretching
1463	1463	1463	1463	CH_3 bending
1414	1412	1412	1413	CH_3 bending
1259	1260	1260	1260	CH_3 bending in Si-CH_3
1070	1075	1075	1071	Si-O-Si stretching
1013	1013	1013	1011	Si-O-Si stretching
795	795	795	794	CH_3 rocking and Si-C stretching in Si-CH_3
754	759	755	756	Si-C stretching in Si-CH_3